Journal of MATERIALS RESEARCH

Article
DOI:10.1557/s43578-023-01166-8

The potential of the mineralized bone allograft block as an appropriate candidate for bone tissue engineering in periodontology

Sara Tabatabaee[1], Mahsa Delyanee[2], Reza Samanipour[3], Amirhossein Tavakoli[4,a)]

[1] Bio-Computing Department, Interdisciplinary Sciences and Technologies Faculty, Tarbiat Modares University, Tehran, Iran
[2] Biomedical Engineering Department, Amirkabir University of Technology, Tehran, Iran
[3] Research and Development Supervisor, Iranian Tissue Product Company, Tehran, Iran
[4] Iranian Tissue Bank and Research Center, Tehran University of Medical Sciences, Tehran, Iran
[a)] Address all correspondence to this author. e-mail: Amirtavakoli.med@gmail.com

Received: 7 March 2023; accepted: 7 September 2023

In this research, an allograft mineralized bone block was processed through decellularizing and lyophilizing after approving the sterility evaluations of the donor. According to SEM images, the block was an interconnected porous structure with pore sizes ranging between 124 and 930 µm which comprised various sizes desirable for bone regeneration. Also, emergence of hydroxyapatite crystals on the scaffold after immersing in simulated body fluid indicated its bioactivity. Furthermore, its mechanical strength was 33.10 ± 0.34 MPa which is suitable for a bone scaffold as load-bearing tissue. The successful decellularization was approved by hematoxylin–eosin staining assay and the scaffold exhibited no cytotoxicity utilizing MTT test. Furthermore, the obtained SEM images after cell seeding as well as the DAPI staining results demonstrated the supporting of cell attachment and proliferation by the scaffold. Therefore, it could be concluded that the prepared allograft mineralized bone block is an appropriate candidate for bone tissue regeneration in periodontology.

Introduction

Bone tissue has significant repairability of several types of fractures, however, in some cases, such as a tumor, trauma, cognitional disabilities, etc., a bone defect may disrupt bone function which could lead to an undesirable impact on the patient's quality of life [1]. These injuries specifically in large defects, would not be recovered by conventional therapeutic strategies [2]. Thus, bone grafts which have been extensively utilized in dentistry and periodontology surgeries should comprise special features such as osteoconductivity, osteoinductivity, and osteogenesity to be considered as an appropriate bone regenerative substitute [3]. Several investigations have been based on achieving an ideal bone graft from different resources and yet it has not been completely accomplished since each introduced scaffold has its specific drawbacks despite the many advantages. Autograft (transplantation from the patient's body to the defective site), as the gold standard treatment for this field and particularly for non-union fractures, has gained desirable outcomes since obviously it would be compatible with the transplanted region compared to other therapeutic methods and contain a variety of growth factors required for bone regeneration like fibroblast growth factor (FGF), bone morphogenic protein (BMP), and transfer growth factor (TGF) which could lead to the stimulation of bone growth and neovascularization. Nevertheless, an autograft is restricted by clinical drawbacks such as donor site morbidity, the probability of further traumas, bleeding, infection, limitations in accessibility, and disruption in the regular skeletal stability of the patient's body [4, 5].

On the other hand, allograft (transplanting from another person who is mainly a cadaver) would provide a structure resembling those of native tissue with no limitations in resources, processability, and storage. Also, the complications of donor site injury after the surgery incision would be resolved in the mentioned strategy [6]. Allograft bone substitutes have been evidenced to cause healing of the bone defects at a similar rate to autografts. It also should be noted that despite the several investigations based on the optimization of synthetic materials for the aim of introducing an appropriate bone graft, the

outcomes could not satisfy the required osteogenic properties as alternatives to natural grafts [7]. Furthermore, xenografting (transplanting from other species) is not capable of biocompatibility as acceptable as grafting from the same species [8].

Based on the pointed features, the clinical utilization of allografts has been developed, however, allogenic products are still struggling with the potential risks of immunogenicity and the transmission of infection, however, it has been stated that the procedure of decellularization is capable of preventing the immune reactions due to eliminating the cell genetic materials such as DNA [9]. Besides the lack of immunogenicity, the bioactive molecules such as desired cytokines and growth factors are not eliminated during the decellularization process which would enable the retained extracellular matrix (ECM) to provide a suitable environment with natural biochemical characteristics [10]. Furthermore, the mineralized content of the acellular bone would not be disrupted and these grafts have demonstrated remarkable structural properties similar to the host tissue such as mechanical strength, osteoconductivity, and osteoinductivity [11]. Therefore, in case of implementation in the damaged site, the resulting ECM could be beneficial for supporting recellularization, osteogenic differentiation of the present stem cells, sufficient osteointegration, and ultimately qualified bone regeneration of the defect [12, 13].

There are various effective chemical agents such as sodium dodecyl sulfate (SDS), Triton X-100, etc. which could be utilized for the decellularization of bone grafts for the aim of reducing the risks of viral contamination. Among them, H_2O_2 as an oxidizing agent can be an appropriate choice. It has been demonstrated that 1 h of H_2O_2 treatment can lead to the reduction of contamination six logs higher the sterility assurance level (SAL) and thus, the probability of a microorganism survival would be less than 10^{-6} [14]. Moreover, although hepatitis C virus (HCV) and human immunodeficiency virus (HIV) are specifically concerned with allografting, it has been reported that rinsing the tissue in ethanol, and lyophilizing would considerably lower the HIV and HCV transmittance possibility. The lyophilizing process is capable of inactivating HIV as well as HCV due to removing the water content of the tissue, preventing the virus's cellular activity and consequently decreasing the transmission risk via contaminated bone marrow or blood [15]. It has been reported that freeze-dried bone grafts are remarkably less probable to induce immunogenic responses in the body rather than the fresh frozen bone grafts [16, 17]. On the other hand, gamma irradiation is considered to be an effective and safe approach for the processed tissue sterilization without notable altering impacts on the biological and mechanical characteristics of bone [18]. According to the previous literature, a dose of 25 kGy can be efficient for inactivating most of the bacterial contamination with a SAL of 10^{-9} which is utilized in the united states tissue banks [19, 20].

In a study by Naishlos et al. [21], 33 patients who had missing teeth in the upper maxilla with extra bone loss were treated by allograft cancellous bone block 6 months before the implant surgery for the aim of bone augmentation. After the implantation, the pink esthetic score (PES)/white esthetic score (WES) was considered as an indication for evaluating the healing process. All patients revealed PES/WES scores more than the clinically acceptable threshold. Therefore, utilizing of allograft bone block resulted in the stability of soft and hard tissue at the implant region in the long term. In a review of literature by Motamedian et al. [22], the success rate of dental implants employing autograft bone blocks versus allograft bone blocks in the human-based studies was compared. The range of the success rate of the implant was 72.8 to 100% and 93.7 to 100% for autograft and allograft, respectively. In another study by Sterio et al., the utilization of allograft cancellous bone for ridge augmentation of 44 patients led to successful implantation of 86.4% (38 of 44) after 6 months and approximately 58% replacement of the graft with vital bone regarding its porous structure which would facilitate the cellular ingrowth and further new tissue formation and also its mechanical compatibility to the defect preventing stress shielding or the graft rejection [23].

Hence, in the following investigation, for the aim of introducing an ideal bone graft regarding the mentioned literature, the procedure of preparing a commercial allograft cancellous bone block (produced by Iranian Tissue Product Company) *"called mineralized bone allograft (MBA) cube"* from donor selection and dissection to various chemically/mechanically treatments for optimum decellularization and terminal sterilization (lyophilization and gamma irradiation) was expressed in detail. Then, the graft was evaluated structurally and biologically in vitro to represent its suitable characteristics and desired capabilities as a promising candidate for bone defect regeneration. The prepared blocks are being used as grafts in dentistry and periodontology for specific purposes such as a dental ridge or alveolar crest augmentation. Regarding the similar characteristics to the native bone tissue, their implantation would lead to the facilitation of the adjacent cellular activities (migration, proliferation, growth, and differentiation to bone cell lines) as well as osteoinduction, osteoconduction, and eventually, new bone formation. Moreover, the mechanical compatibility of the grafts to the defect area would prevent loosening, breaking, and further rejection of the graft. The mentioned suitable characteristics for application in dental bone defects will be evaluated in the following investigation.

Result and discussion

Structural and mechanochemical characterizations

A critical role is performed by the scaffold's pores in bone regeneration since it facilitates the nutrition and oxygen exchange as well as the removal of the undesired products resulting in appropriate vascularization and new bone tissue formation [24]. The structural pores were evaluated via SEM images of the blocks'

surface (Fig. 1) and the quantitative analysis results via image-J based on the obtained images as well as the scaffold's porosity according to BET analysis results are gathered in Table 1. Also on this basis, the scaffold was porous with interconnected pores which is an essential factor in bone tissue engineering due to its influence on efficient cell growth [25, 26]. The SEM image processing via image-J indicated the allograft block contained pores with size ranges between 120 and 930 μm with a mean pore size of 375 ± 16 μm. It has been stated that pore sizes smaller than 300 μm are desirable for initial cellular migration and infiltration as well as the acceleration of osteochondral ossification. On the other hand, pore sizes greater than 300 μm are required for the facilitation of vascularization and ingrowth of bone tissue [27]. Furthermore, according to the in vitro studies, the bone scaffold's porosity of more than 70% would result in optimum osteogenic proliferation and differentiation which is in line with the obtained result (76.6 ± 0.8%) [28]. Also, the mentioned amount would be desirably efficient in replicating the structural porosity of cancellous bone which concerning the literature is reported to be 75%-85% [29]. Regarding the previous investigations, it could be concluded that the resulting pore size ranges as well as the amount of porosity are suitable for bone augmentation on every mentioned aspect.

The bioactivity potential of the MBA blocks was analyzed regarding the apatite formation 3 and 7 days after immersing in SBF. Calcium phosphates are considered the main minerals found in human bone and have a direct impact on the implant bioactivity (desirable interaction with the native tissue) through their local concentration increase and stimulation of the bone formation, i.e., they would increase the expression of osteo-differentiation markers such as alkaline phosphatase, osteopontin, collage type I, etc., and enhance the ECM proteins adsorption which would consequently, improve the cellular adhesion and tissue formation [30–33]. Therefore, the presence of calcium phosphate would lead to promoting osteoinduction (inducing the differentiation of the progenitor cells to osteoblastic cell lines) and the osteoconduction (growth of bone on the scaffold surface) capability of the graft. HA as the major inorganic component of bone is naturally derived from calcium phosphates and has been broadly utilized as an indicator for the scaffold bioactivity. The obtained SEM images could be observed in Fig. 2(a and b). The formation of calcium phosphate sinters on the block's surface is obvious. EDX spectra of the blocks were obtained 7 days after soaking in SBF to evaluate the Ca/P atomic ratio of the formed sinters on the scaffolds' surface [Fig. 2(c)]. According to the plot, the ratio was approximately equal to 1.7 which reveals the stochiometric ratio of HA [34]. Therefore, the results demonstrated the biomineralization of the blocks in SBF as an indication of their bioactivity. Also, it could be evidenced that the prepared scaffold would lead to osteoinduction, osteoconduction, and eventually new bone formation in case of implantation in the bone defect [35, 36].

The quality of bone is a general factor which impacts both structural and material characteristics resulting in preventing fracture occurrence [37, 38]. As stated in the literature, structural properties such as macroscopic and microscopic geometry are not strongly reliable to estimate the risk of fracture and should be considered along with material properties including the composition as well as the arrangement of principal bone elements [39]. The mentioned information at the molecular level could be provided by FTIR spectroscopy. According to the FTIR spectroscopy of the mineralized bone block 1 and 7 days after soaking in SBF (Fig. 3), a sharp peak can be observed at 1035 cm^{-1} which is related to the nonstoichiometric apatite (HPO_4^{2-} and/or CO_3^{2-}) indicating the scaffold mineral maturity. Also, crystallinity is generally correlated with mineral maturity which in this case, there is a peak at 603 cm^{-1} that could be an index of hydroxyapatite (HA) crystallinity. Another factor that affects the mineral maturity is the substitution amount in the HA crystal lattice. Carbonate peak, as the most frequent substitute in the bone and an indicative factor for bone remodeling activity could be seen at 869 cm^{-1}. On the other hand, the chemistry of cross-linking is a critical property of collagen type I maturity specifically in mineralized bone which would lead to its viscoelasticity to fibrillar matrices and tensile strength. The band of amide I is used as an index in the mentioned regard. Herein, the 1664 cm^{-1} can be associated with the existence of reducible cross-links of collagen based on the previous investigation [40, 41]. Furthermore, regarding the obtained spectra, no significant shifts in the existing peaks were observed on day 7 after immersing in SBF compared to the first day. The apatite formation which was indicated in EDX spectra could not be demonstrated by FTIR as a qualitative assay since the hydrogen

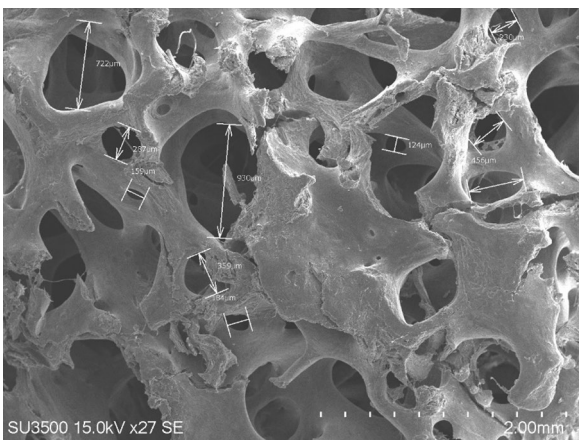

Figure 1: SEM images of the bone blocks.

TABLE 1: Microstructural characteristics of the bone blocks.

Minimum observed pore size (μm)	Maximum observed pore size (μm)	Mean pore size (μm)	% porosity
120	930	375 ± 16	76.6 ± 0.8

bonding between the formed apatite and the bone surface can be covered in the broad peak of -OH of the spectrum and may not express a definitive statement on this basis {Posner, 1985 #7}. Overall, the FTIR spectrum of the prepared scaffold could indicate the desirable allograft bone quality concerning its maturity both in the mineral phase and the existing collagen as well as its capacity for bone remodeling.

The mechanical strength of a bone scaffold as a load-bearing tissue is a critical factor with a significant impact on its efficiency in case of implanting in the body and specifically in the dental area regarding the high applied mechanical loads [42, 43]. Moreover, the regulative effect of mechanical characteristics in positive manipulating of cellular as well as tissue level host responses has been evidenced [44, 45]. The mechanoregulatory impact plays a key role in the growth of bone tissue due to the replication of the natural mechanical forces of bone which would be transferred to the present cells and stimulate the osteogenic differentiation [46]. For the aim of investigating the scaffold's behavior under the mechanical compression similar to what occurred in case of implantation in the bone defect, the samples were loaded by a 25 kN load cell. The stress–strain curve of the bone block under the pressure with a rate of 1 mm/min is presented in Fig. 4. Also, the obtained mechanical properties from the plot are shown in Table 2. According to the results, the compressive modulus and the ultimate compressive strength of the samples are reported to be 33.10 ± 0.34 MPa and 3.36 ± 0.15 MPa respectively. Based on the previous investigations, a compressive modulus between 1.5 and 45 MPa appears to be appropriate for utilizing cancellous bone which is sufficient for dental bone augmentation (such as a ridge or alveolar crest) [47, 48]. Although, the mechanical strength of a scaffold is conflicted by its porosity and these structural properties are in inverse relation to each other, according to the literature, the mentioned ideal amount of mechanical strength is associated with a porosity between 60 and 90% and a mean pore size more than 150 μm which is in line with our outcomes regarding the SEM images of the graft microstructure [49, 50].

The reason behind the relatively high compressive strength of the allograft bone blocks can be the retaining of its mineralized content such as HA and not disrupting its composition during the production process. Follet et al. [41], took calcaneus bone samples from 20 cadavers and after adapting the outputs of radio micrographs and compression tests revealed that there is a linear correlation between the degree of bone mineralization and compressive modulus as well as maximum compressive strength. This enhancement can be justified with mineralization contents such as HA acting as crack resistance via bridging and deflection. Obviously, numerous microcracks may appear on the bone structure during its shelf life. In case of a lack of adequate regenerative capability of bone, the microcracks would propagate and form larger cracks caused in occurring serious bone fractures [51]. As was noted, contents such as HA are able to play a role as a crack bridge. Consequently, the microcracks would be crossed and deflected from their main direction and blocked to be more propagated and thus the growth of the cracks would require more stress [52]. Considering the compressive test results, it can be claimed that the mechanical strength of the mineralized bone blocks was enhanced due to the retaining of the mineralized content in their composition and the mechanical strength of the graft was efficient for applying in dental bone defects [53].

Biological analysis

The main concern of using allograft products is the risk of immune reactions and rejection of the implant by the host body which could be eliminated through removal of the graft's genetic materials and decellularization [54]. In this project, for the aim of validating the decellularization protocol, H&E staining of the existing cell nuclei was performed. The images of H&E staining of the acellular bone blocks can be seen in Fig. 5(a and b). The submitted bone showed woven bony trabeculae which were composed of osteoid matrices, bony lamellae, some osteocytes with pyknotic nuclei, and empty lacunae accompanied by sporadic haversian system formation. Also, it can be seen that the natural matrix of bone has been preserved after the decellularization process [55, 56]. Therefore, the decellularization of the blocks was accomplished and based on the references and the probability of evoking any immune reaction in case of implanting would be negligible [57].

For the aim of assessing the viability of hBM-MSCs, and predicting the biocompatibility of the blocks in case of implantation in the defect area, MTT assay was carried out 72 h after culturing [Fig. 5(c)]. Regarding the bar chart, although the cellular viability on the bone block with 92.74 ± 0.18% was significantly lower than the cell viability of TCP (p value < 0.05), it was acceptable for approving the block cytocompatibility. The reason behind this result could be using of direct MTT and the absorbance of the color by the scaffold which consequently would affect the light absorption and the reported viability [58]. The output complied with previous research; as Kouhestani et al. [59], reported the MTT value of freeze-dried bone allograft was notably higher than microporous biphasic calcium phosphate granules as a synthetic bone scaffold. This outcome could be interpreted by surface characteristics resembling the native

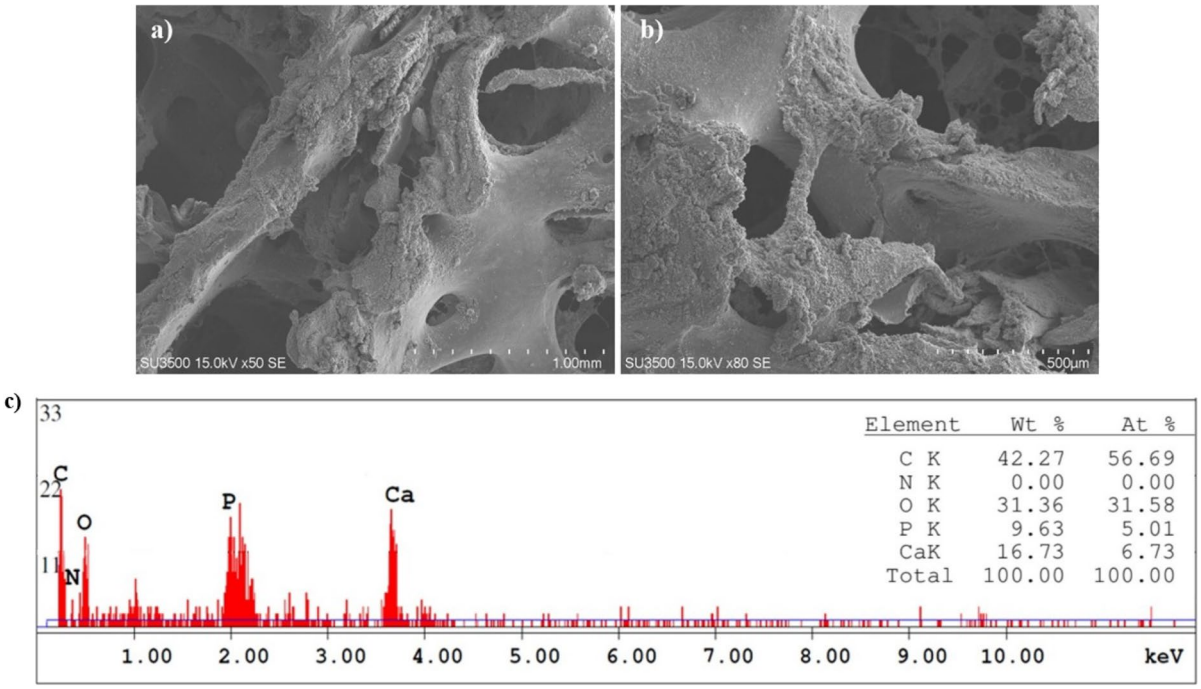

Figure 2: The SEM images of the blocks presenting their bioactivity (a) 3 days and (b) 7 days after soaking in SBF. (c) The EDX spectra of the prepared block 7 days after soaking in SBF.

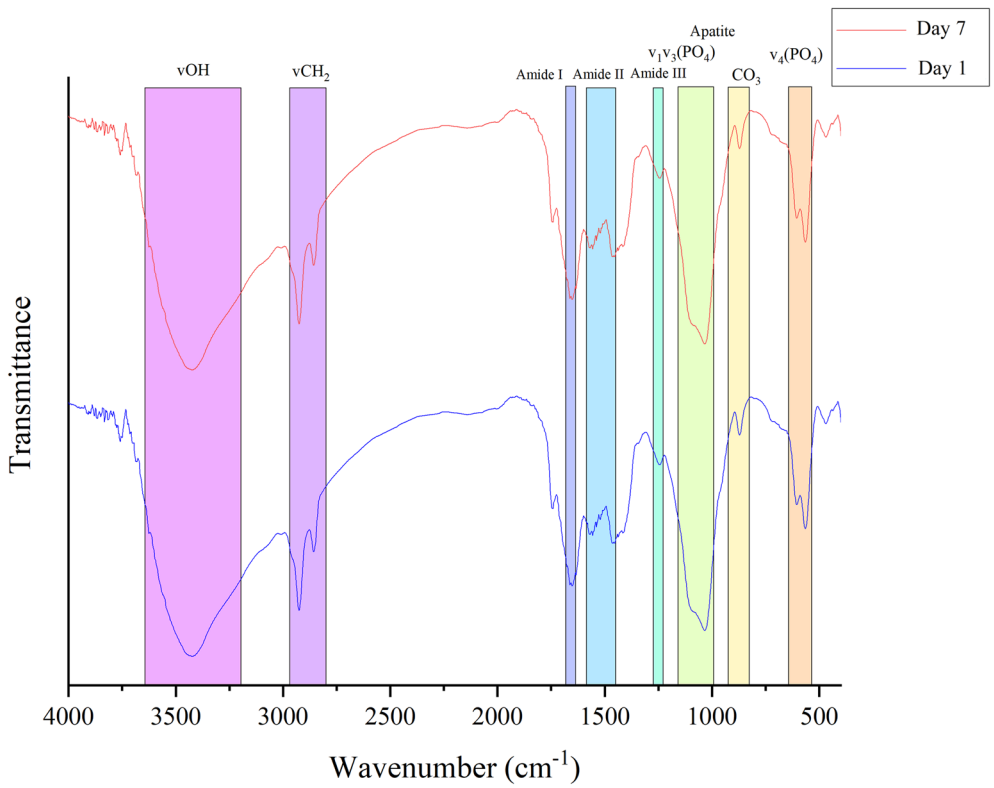

Figure 3: FTIR result of the bone block sample 1 and 7 days after soaking in SBF.

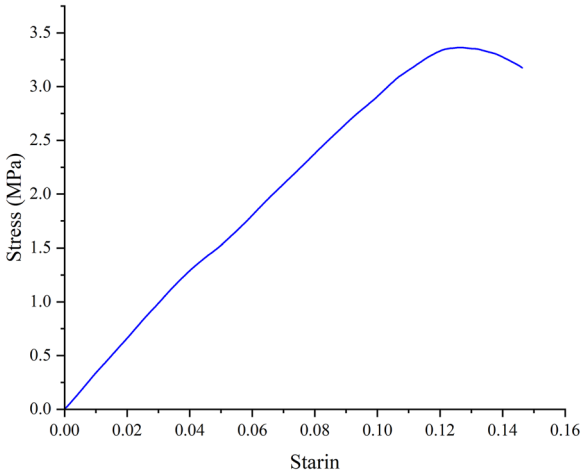

Figure 4: Stress–strain curve of the bone blocks.

TABLE 2: Mechanical characteristics of the bone blocks.

Compressive modulus (MPa)	Ultimate compressive strength (MPa)	Stress at the crack (MPa)	Failure strain
33.10 ± 0.34	3.36 ± 0.15	3.17 ± 0.21	0.150 ± 0.006

bone tissue (the mineral phase and other components such as collagen as indicators for desirable bone quality which was discussed in FTIR and EDX results) leading to cytocompatibility and improvement of the cellular viability. Moreover, another feature that should be noted is the interconnectivity of the pores (observed in SEM images). Based on the literature, an interconnected scaffold would permit the oxygen and other nutrients infusion as well the waste product diffusion which would obviously, cause the enhancement of the cell viability [60]. Hence, the biocompatibility of the bone blocks and their cellular safety in case of implantation in the bone defect area were observed.

The SEM images of the cultured hBM-MSCs on bone blocks were obtained after 1, 7, and 14 days to assess the scaffold capability of providing an appropriate environment for cellular activities (Fig. 6). The scaffold was evidenced to be able to facilitate the cell attachment and growth even after 1 day since an intact cellular migration and locating as well as adhesion on the surface of the blocks could be observed vividly. The interaction between the scaffold and the cells became more intense since in the images of days 7 and 14, an expansion and elongation of cellular appendages is obvious. The improvement of cellular adhesion in the bone blocks can be interpreted by the presence of an appropriate pore size range in the block's structure which would lead to enhanced cellular locating through the scaffold [61]. As has been stated in the literature, the porous microstructure of the graft is critical for promoting cell migration rate and improving the binding between cells and the scaffold through increasing the available surface area which would result in enhancing cellular adhesion. There should be a balance between the pore size and the surface area, as the less pore size (less than 300 μm) would result in the more surface area and more scaffold ligands to bind to the cells, and contrarily, an increase of the individual pore size would eliminate the cellular struggling to migrate. Regarding the information obtained from the bone blocks microstructure, it was able to prepare the mentioned desirable criteria for cellular activities [62, 63].

On the other hand, the retained mineralized content such as HA could result in more surface roughness and more cellular attachment [64]. As Bhumiratana et al. [65], have revealed the addition of the HA to the composition of a scaffold would result in the improvement of its surface roughness, and consequently, the more surface roughness would cause more cell trapping and attachment. Furthermore, cell attachment is remarkably associated with the capacity of absorbing ECM proteins which could be promoted via the presence of calcium phosphate phase and specifically HA which according to the aforementioned EDX results, it has been evidenced [66].

Consequently, it could be claimed that the prepared scaffold would be suitable for the facilitation of cellular migration, attachment, and ingrowth which would further lead to optimum tissue ingrowth and new bone tissue formation [50].

DAPI staining was utilized to evaluate the proliferation of the cultured cells on the scaffolds and TCP as the control group. Figure 7(a and b) show the images of DAPI staining of the cells on the bone blocks after 7 and 14 days compared to the control sample [Fig. 7(c and d)]. Also, the outcome of the DAPI image processing by image-J is presented in Fig. 7(e). Regarding the bar chart, a significant increase (p value < 0.001) in the cell adhesion number occurred after 7 days which also is noticeable in the images. Moreover, it should be noted that the cellular proliferation was significantly higher on the bone blocks in comparison with TCP on both day 7 and 14. According to the data provided by DAPI staining, it can be claimed that the bone blocks established an appropriate interaction with the seeded cells resulting in their remarkable proliferation. It is noteworthy that it has been previously evidenced that the mineralization of a bone scaffold would enhance its cellular interactions such as adhesion and proliferation which was approved by EDX results [42]. In a study by Ryu et al. [67], a synthetic scaffold composed of poly (methyl methacrylate) (PMMA), paper, bioglass, Ti, and polydopamine which was mineralized using SBF showed better proliferation of the pre-osteoblasts than its non-mineralized form due to its suitable environment for ECM generation of the cells. The ECM plays a role as the medium for the attachment of the proliferated cells and also facilitates the cellular communications leading to further facilitation of the defective bone healing process.

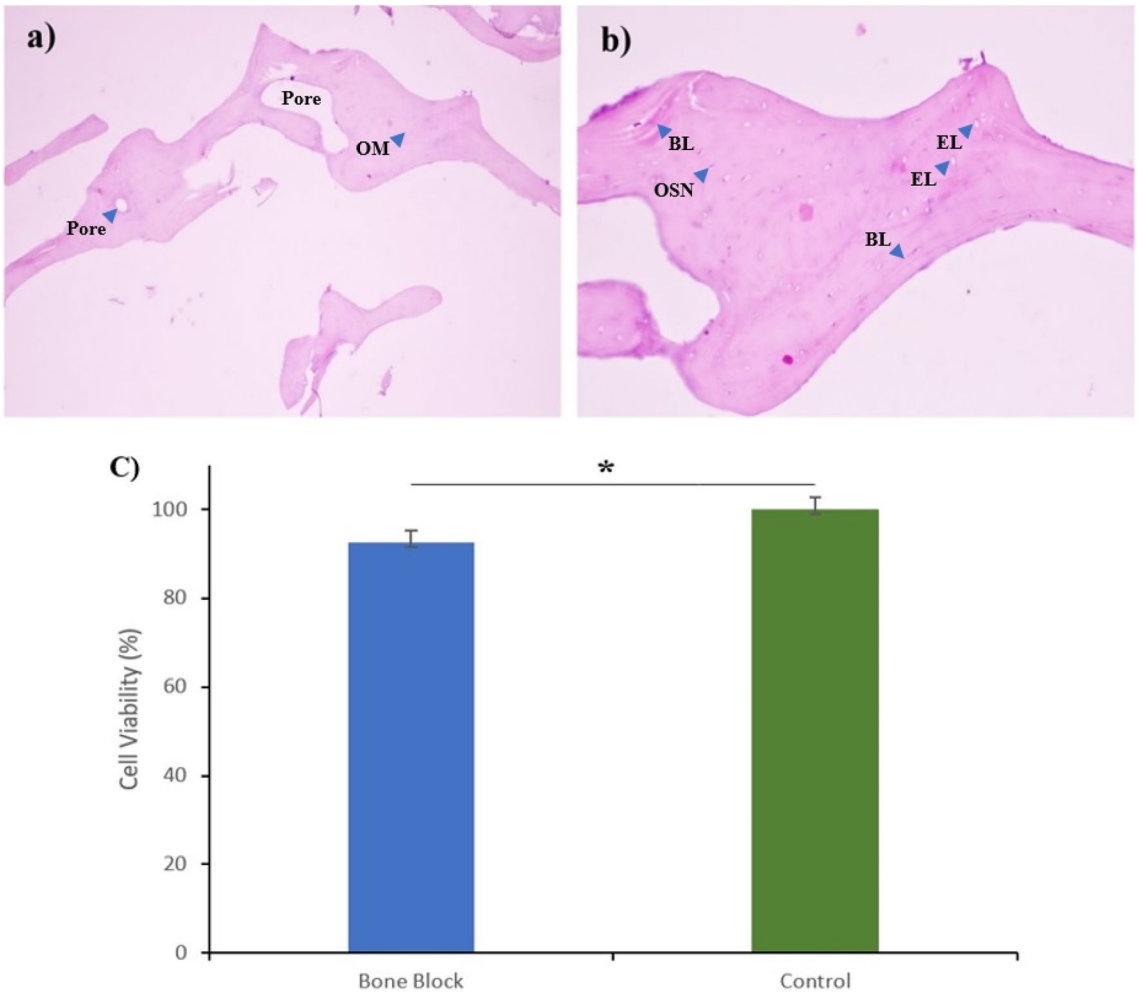

Figure 5: H&E staining images of the bone blocks; (a) 4 × and (b) 10 × magnifications, indicating bony pores, OM: osteoid matrices, BL: bony lamellae, OSN: osteocytes with pyknotic nuclei, EL: empty lacunae; (c) MTT results of the bone blocks. (*: p value < 0.05).

Conclusion

The aim of this project was to introduce a desirable bone substitute for periodontology. FTIR spectroscopy revealed the mineral maturity and crystallinity of the bone blocks. Also, the carbonate peak as an index for the bone remodeling ability of the graft was distinguished. The SEM images showed the interconnected porous structure with an appropriate pore size range for bone tissue regeneration. The mechanical characteristics of the scaffolds were in line with the suggested amounts for application in cancellous bone. The EDX mapping of the soaked scaffolds in SBF demonstrated the presence of HA on their surface and thus approved their bioactivity, osteoinductivity, and osteoconductivity. The H&E staining of the blocks revealed the successful decellularization of the samples and the low probability of causing any immune reaction in the host tissue. The MTT assay confirmed the cytocompatibility of the block. Also, based on the SEM and DAPI staining images, the block surface was a desirable microenvironment for the cells to attach, proliferate and generate the new ECM. Considering the obtained results, the prepared allograft decellularized bone blocks could be a suitable scaffold for bone regeneration and healing the bone defects.

Methodology

Preparation of the bone blocks

After completion of donor screening and assuring of the lack of any specific bioburden (bacteria, yeast, mold, etc.), the tissue was examined in case of sterility (HIV, HCV, hepatitis B virus (HBV), Human T-lymphotropic virus-1 (HTLV-1), etc.). If the outcome of the sterility assay was negative, the cancellous bone tissue was dissected for removing any additional tissue. The achieved pure bone tissue was cut into block-shaped structures with identical sizes of $10 \times 10 \times 10$ mm^3. The blocks were then mechanically washed through the following process: washing with DI water on the centrifuge for 30 min, ultrasonically radiating for 20 min,

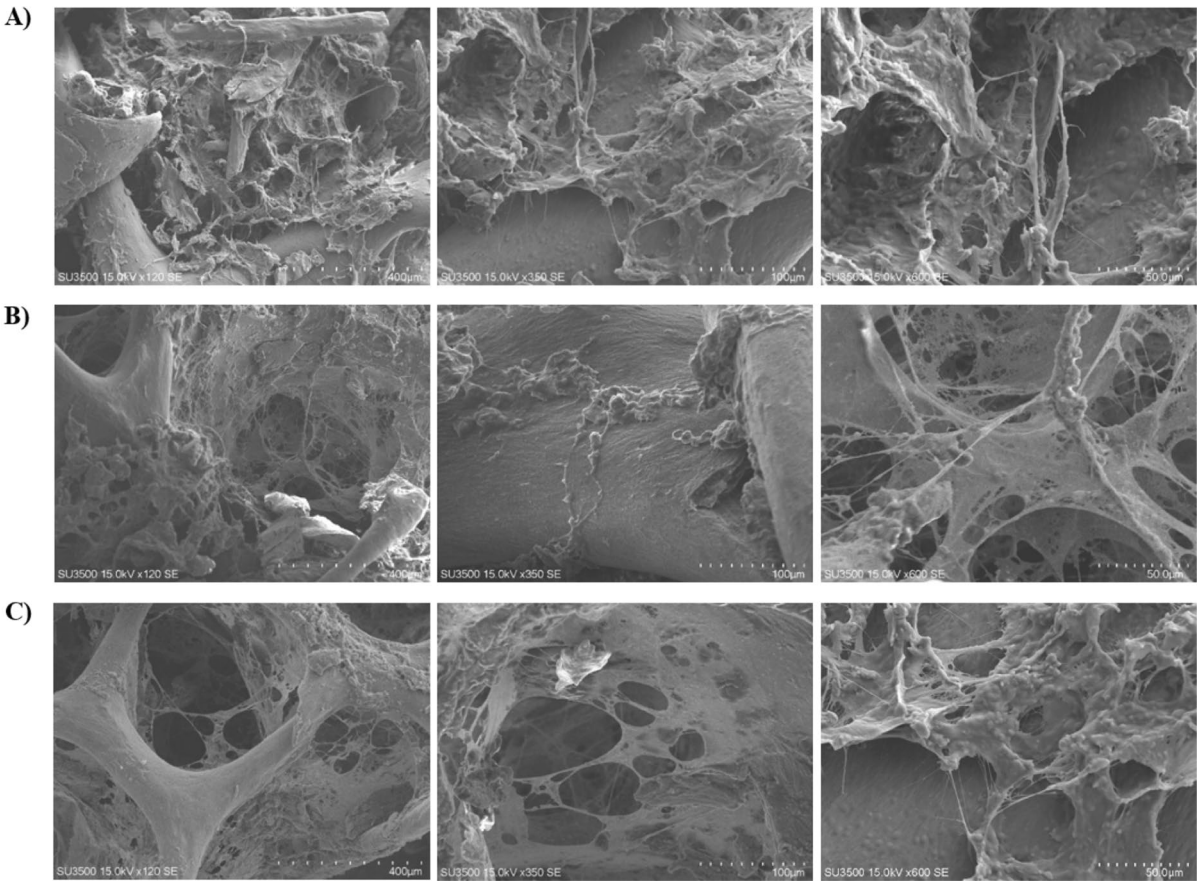

Figure 6: SEM images of the hBM-MSCs cultured on the bone blocks; (A) 1, (B) 7, and (C) 14 days after culturing with different magnifications.

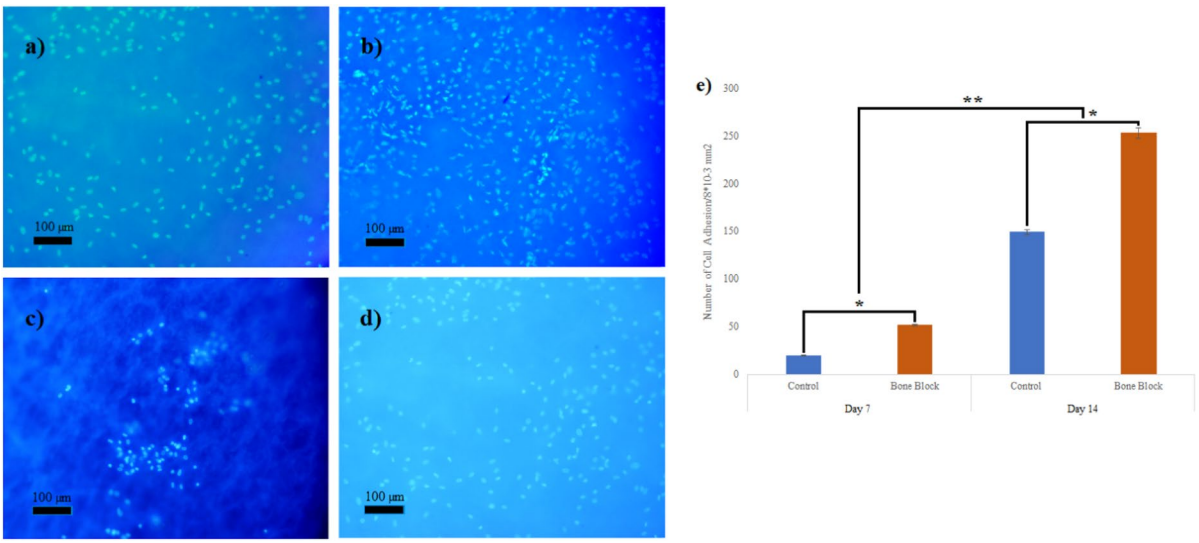

Figure 7: DAPI staining images of the cultured cells on bone block after **a** 7 days and **b** 14 days and TCP as the control sample after **c** 7 days and **d** 14 days. **e** Quantitative difference analysis of the cultured cells on days 7 and 14 according to the DAPI staining images, *presents p value < 0.05 and **p value < 0.001.

washing with ethanol 70% for 15 min on the shaker, Final washing with DI water on the shaker for 5 min. At this stage, H_2O_2 (5%; Sigma-Aldrich, USA) was utilized for 8 h to decellularize the blocks. After the treatment, the grafts were washed with DI water on the shaker (30 min) and centrifuge (15 min). The blocks were lyophilized using a freeze-dryer (Alpha 2–4 LDplus, Martin

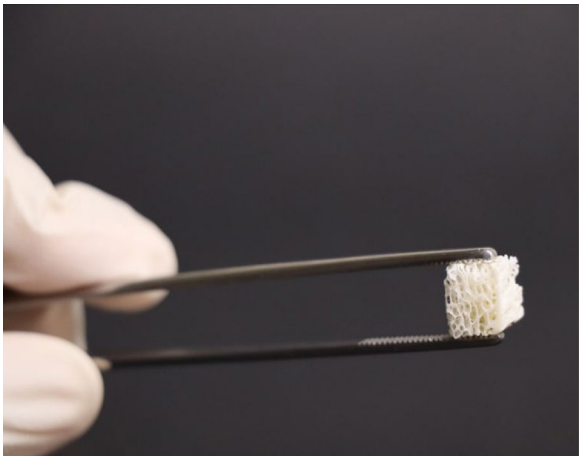

Figure 8: The prepared allograft bone blocks with the size of 10 × 10 × 10 mm^3.

Christ, Germany) for 48 h. Finally, the resulting bone blocks were gamma irradiated with a dose of 25 kGy for 12 h. The prepared bone blocks could be observed in Fig. 8.

Structural and mechanochemical characterizations

The blocks were gold coated for observing their microstructure by scanning electron microscopy (SEM; XL30, Philips). Then, the image-J software was used to process the SEM images and measure the samples' pore size. Also, the porosity of the scaffold was evaluated using the Nauer–Emmett–Teller (BET) method (Gemini II 2370 micromeritics). For the aim of investigating the bioactivity of the samples, the blocks were immersed in the simulated body fluid (SBF; 1x) at 37 °C for 3 and 7 days, followed by air-drying for 24 h. The formed crystals on the samples' surface were studied using SEM connected to an energy-dispersive X-ray analyzer (EDX; Rontec) in case of analyzing the Ca/P ratio as well as the morphology of the crystals. Fourier-transform infrared spectroscopy (FTIR) (PerkinElmer, Frontier) was used to assess the chemical composition of the prepared blocks on a KBr-diluted medium, in a range between 4000 and 400 cm^{-1}, with a scan speed as well as resolution of 32 scan/min and 1 cm^{-1}, respectively. Also, A universal testing machine (H10KS; Hounsfield) was utilized to examine the compressive strength of the scaffolds. In the mentioned test, a 25 kN load cell with a rate of 1 mm/min was compressed on the blocks until the appearance of the first crack for obtaining the stress–strain curve. The blocks' compressive modulus was reported based on the linear region slope of the stress–strain plot.

Cellular analysis

For the aim of validation of the decellularization process, hematoxylin and eosin (H&E) colorimetric staining was used. In this regard, the blocks were fixed by 10% (v/v)-buffered formalin for 24 h at ambient temperature. At this stage, they were decalcified employing 10% nitric acid for 21 days and then dehydrated by graded ethanol. Finally, the samples were placed in paraffin, cross-sectioned at the thickness of 5 µm, and stained by hematoxylin (Sigma-Aldrich, USA) and eosin (Sigma-Aldrich).

Also, human bone marrow mesenchymal stem cells (hBM-MSCs) were selected for evaluating the blocks' cytotoxicity. The cell culture medium consisted of Dulbecco's modified eagle medium F12 (DMEMF12; Invitrogen) medium, 10% (v/v) fetal bovine serum (FBS; Gibco), and 1% antibiotic penicillin/streptomycin (Sigma-Aldrich). The blocks were sterilized using ethanol 70%, soaked in phosphate buffer saline (PBS; Sigma-Aldrich), and positioned on each side under radiation of ultraviolet (UV) for 20 min. At this point, 8×10^3 cells were loaded on the grafts in 24-well culture plates and the plates were placed in a 5% CO_2 incubator at 37 °C. The cell viability assessment was performed using MTT colorimetric assay after 72 h [68]. In brief, the culture medium was removed and 100 µL of MTT solution (5 mg/mL in PBS) was poured into the wells and incubated for 7 h. After removing the medium, dimethyl sulfoxide (DMSO; Sigma-Aldrich) was employed to dissolve the crystals of formazan. A microplate reader (ELISA reader; ELX808, BioTek) evaluated the optical absorbance of the samples at 540 nm. In this assay, the cells cultured on the tissue culture plate (TCP) were the positive control group.

Furthermore, the cellular adhesion was observed by SEM 1, 7, and 14 days after culturing. For this purpose, 2.5% glutaraldehyde (GA; Sigma-Aldrich) was used to fix the cells for 1 h, followed by PBS washing several times, dehydrating with graded ethanol, and gold coating.

In order to evaluate the cellular proliferation capability of the bone blocks, they were seeded by hBM-MSCs and 4′,6-diamidino-2-phenylindole (DAPI) staining was performed at 7 and 14 days after culturing. On this basis, the blocks were stained by 1 mg/ml of DAPI solution at the mentioned time points. Then, the samples were rinsed in PBS and a Nikon Eclipse TI fluorescence microscope was used to capture the images. In this evaluation, the cultured cells on TCP were considered as the control group. The images were analyzed quantitatively by image-J software.

Statistical analysis

The outputs were reported as mean ± standard deviation (SD). At least 3 samples were assessed for each investigation which was run at least 3 times. The statistical analysis was performed using one-way analysis of variance (ANOVA) employing SPSS 16.0 software (SPSS). *P* values less than 0.05 were stated as significant.

Acknowledgments

We sincerely thank Forensic Medicine Center of Tehran for their valuable cooperation in preparing the raw material and basic information needed to write this article.

Funding

This research was financially supported by Iranian Tissue Product (ITP) Company.

Data availability

The authors confirm that the data supporting the findings of this study are available within the article.

Declarations

Conflict of interest The authors report there are no competing interests to declare.

Ethical approval

All human rights were concerned in this research. All the tissues (as the raw material) were utilized after obtaining the written consent of the next of kin. Also, this project was approved by research ethics committee of Imam Khomeini Hospital Complex – Tehran University of Medical Sciences with the approval ID of IR.TUMS.IKHC.REC.1399.354.

Consent for publication

The verbal consent of the next of kin was obtained for the data publication provided that the donor's name would not be disclosed.

References

1. P. Wang, L. Zhao, J. Liu, M.D. Weir, X. Zhou, H.H. Xu, Bone tissue engineering via nanostructured calcium phosphate biomaterials and stem cells. Bone Res. **2**(1), 1 (2014)
2. A. Bigham-Sadegh and A. Oryan: Basic concepts regarding fracture healing and the current options and future directions in managing bone fractures(1742–481X (Electronic)).
3. H.-S. Sohn, J.-K. Oh, Review of bone graft and bone substitutes with an emphasis on fracture surgeries. Biomater. Res. **23**(1), 9 (2019)
4. J.D. Cooper, T.J. Dekker, J.J. Ruzbarsky, L.A. Pierpoint, R.W. Soares, M.J. Philippon, Autograft versus allograft: the evidence in hip labral reconstruction and augmentation. Am. J. Sports Med. **49**(13), 3575 (2021)
5. H. Tebyanian, M.H. Norahan, H. Eyni, M. Movahedin, S.J. Mortazavi, A. Karami, M.R. Nourani, N. Baheiraei, Effects of collagen/β-tricalcium phosphate bone graft to regenerate bone in critically sized rabbit calvarial defects. J. Appl. Biomater. Funct. Mater. **17**(1), 2280800018820490 (2019)
6. M. Meskinfam, S. Bertoldi, N. Albanese, A. Cerri, M.C. Tanzi, R. Imani, N. Baheiraei, M. Farokhi and S. Farè: Polyurethane foam/nano hydroxyapatite composite as a suitable scaffold for bone tissue regeneration(1873–0191 (Electronic)).
7. W. Wang and K.W.K. A. Neishabouri, A. Soltani Khaboushan, F. Daghigh, A.-M. Kajbafzadeh and M. Majidi Zolbin: A review (2452–199X (Electronic)).
8. T. Lu, B. Yang, R. Wang, C. Qin, Xenotransplantation: current status in preclinical research. Front. Immunol. (2020). https://doi.org/10.3389/fimmu.2019.03060
9. A. Neishabouri, A. Soltani Khaboushan, F. Daghigh, A.-M. Kajbafzadeh and M. Majidi Zolbin: Decellularization in Tissue Engineering and Regenerative Medicine: Evaluation, Modification, and Application Methods. Frontiers in Bioengineering and Biotechnology **10**, (2022).
10. H.A.-O. Amirazad, M.A.-O. Dadashpour and N.A.-O. Zarghami: Application of decellularized bone matrix as a bioscaffold in bone tissue engineering(1754–1611 (Print)).
11. E. Gruskin, B.A. Doll, F.W. Futrell, J.P. Schmitz, J.O. Hollinger, Demineralized bone matrix in bone repair: history and use. Adv. Drug Deliv. Rev. **64**(12), 1063 (2012)
12. N.A. Ebraheim, H. Elgafy, R. Xu, Bone-graft harvesting from iliac and fibular donor sites: techniques and complications. JAAOS-J. Am. Acad. Orthopaedic Surg. **9**(3), 210 (2001)
13. Z. Amini, R. Lari, A systematic review of decellularized allograft and xenograft-derived scaffolds in bone tissue regeneration. Tissue Cell **69**, 101494 (2021)
14. B. McEvoy, N.J. Rowan, Terminal sterilization of medical devices using vaporized hydrogen peroxide: a review of current methods and emerging opportunities. J. Appl. Microbiol. **127**(5), 1403 (2019)
15. J.M. Wagner, N. Conze, G. Lewik, C. Wallner, J.C. Brune, S. Dittfeld, H. Jaurich, M. Becerikli, M. Dadras, K. Harati, Bone allografts combined with adipose-derived stem cells in an optimized cell/volume ratio showed enhanced osteogenesis and angiogenesis in a murine femur defect model. J. Mol. Med. **97**, 1439 (2019)
16. D.M. Strong, G.E. Friedlaender, W.W. Tomford, D.S. Springfield, T.C. Shives, H. Burchardt, W. Enneking, H.J. Mankin, Immunologic responses in human recipients of osseous and osteochondral allografts. Clin. Orthopaedics Related Res. **326**, 107 (1996)
17. D.M. Ehrler, A.R. Vaccaro, The use of allograft bone in lumbar spine surgery. Clin. Orthopaedics Related Res. **371**, 38 (2000)
18. A. Kaminski, A. Jastrzebska, E. Grazka, J. Marowska, G. Gut, A. Wojciechowski, I. Uhrynowska-Tyszkiewicz, Effect of gamma irradiation on mechanical properties of human cortical bone: influence of different processing methods. Cell Tissue Banking **13**, 363 (2012)

19. W. Wei, Y. Liu, X. Yang, S. Tian, C. Liu, Y. Zhang, Z. Xu, B. Hu, Z. Tian, K. Sun, Fractionation of 50 kGy electron beam irradiation: effects on biomechanics of human flexor digitorum superficialis tendons treated with ascorbate. J. Biomech. **46**(4), 658 (2013)
20. A. Pruss, M. Kao, U. Gohs, J. Koscielny, R. von Versen, G. Pauli, Effect of gamma irradiation on human cortical bone transplants contaminated with enveloped and non-enveloped viruses. Biologicals **30**(2), 125 (2002)
21. S. Naishlos, E. Zenziper, H. Zelikman, J. Nissan, S. Mizrahi, G. Chaushu, S. Matalon, L. Chaushu, Esthetic assessment succeeding anterior atrophic maxilla augmentation with cancellous bone-block allograft and late restoration loading. J Clin. Med. **10**(20), 4635 (2021)
22. S.R. Motamedian, M. Khojaste, A. Khojasteh, Success rate of implants placed in autogenous bone blocks versus allogenic bone blocks: a systematic literature review. Annals Maxillofacial Surg. **6**(1), 78 (2016)
23. T.W. Sterio, J.A. Katancik, S.B. Blanchard, P. Xenoudi, B.L. Mealey, A prospective, multicenter study of bovine pericardium membrane with cancellous particulate allograft for localized alveolar ridge augmentation. Int. J. Periodontics Restor. Dent. (2013). https://doi.org/10.11607/prd.1704
24. H. Mohammadi, M. Sepantafar, N. Muhamad, A. Bakar Sulong, How does scaffold porosity conduct bone tissue regeneration. Adv. Eng. Mater. **23**(10), 2100463 (2021)
25. S. Tabatabaee, N. Baheiraei, M. Salehnia, Fabrication and characterization of PHEMA–gelatin scaffold enriched with graphene oxide for bone tissue engineering. J. Orthopaedic Surg. Res. **17**(1), 216 (2022)
26. S.G. González, M.D. Vlad, J.L. López, E.F. Aguado, Novel bio-inspired 3D porous scaffold intended for bone-tissue engineering: Design and in silico characterisation of histomorphometric, mechanical and mass-transport properties. Mater. Design **225**, 111467 (2023)
27. C.M. Murphy and F.J. O'Brien: Understanding the effect of mean pore size on cell activity in collagen-glycosaminoglycan scaffolds(1933–6926 (Electronic)).
28. J. Jiao, Q. Hong, D. Zhang, M. Wang, H. Tang, J. Yang, X. Qu and B. Yue: Influence of porosity on osteogenesis, bone growth and osteointegration in trabecular tantalum scaffolds fabricated by additive manufacturing *Frontiers in Bioengineering and Biotechnology.* 11, (2023).
29. E. Novitskaya, S. Chen Py Fau - Lee, A. Lee S Fau - Castro-Ceseña, G. Castro-Ceseña A Fau - Hirata, V.A. Hirata G Fau - Lubarda, J. Lubarda Va Fau - McKittrick and J. McKittrick: Anisotropy in the compressive mechanical properties of bovine cortical bone and the mineral and protein constituents(1878–7568 (Electronic)).
30. S. Bose, S. Tarafder, Calcium phosphate ceramic systems in growth factor and drug delivery for bone tissue engineering: a review. Acta Biomaterialia **8**(4), 1401 (2012)
31. B. Ben-Nissan, *Advances in calcium phosphate biomaterials* (Springer, Berlin, 2014)
32. E. Fujii, M. Ohkubo, K. Tsuru, S. Hayakawa, A. Osaka, K. Kawabata, C. Bonhomme, F. Babonneau, Selective protein adsorption property and characterization of nano-crystalline zinc-containing hydroxyapatite. Acta Biomaterialia **2**(1), 69 (2006)
33. T. Komori, *Regulation of osteoblast differentiation by Runx2, in Osteoimmunology: Interactions of the Immune and skeletal systems II* (Springer, Boston, 2010), p.43
34. C.-H. Lin, Y.-S. Chen, W.-L. Huang, T.-C. Hung, T.-C. Wen, Hydroxyapatite formation with the interface of chitin and chitosan. J. Taiwan Inst. Chem. Eng. **118**, 294 (2021)
35. A. Ullah, M.K. Haider, F.-F. Wang, S. Morita, D. Kharaghani, Y. Ge, Y. Yoshiko, J.S. Lee, I.S. Kim, "Clay-corn-caprolactone" a novel bioactive clay polymer nanofibrous scaffold for bone tissue engineering. Appl. Clay Sci. **220**, 106455 (2022)
36. J. Jeong, J.H. Kim, J.H. Shim, N.S. Hwang, C.Y. Heo, Bioactive calcium phosphate materials and applications in bone regeneration. Biomater. Res. **23**(1), 1 (2019)
37. J.H. Cole and M.C. van der Meulen: Whole bone mechanics and bone quality(1528–1132 (Electronic)).
38. S.K. Venkatraman, R. Choudhary, N. Vijayakumar, G. Krishnamurithy, H.R.B. Raghavendran, M.R. Murali, T. Kamarul, A. Suresh, J. Abraham, S. Swamiappan, Investigation on bioactivity, mechanical stability, bactericidal activity and in-vitro biocompatibility of magnesium silicates for bone tissue engineering applications. J. Mater. Res. (2022). https://doi.org/10.1557/s43578-021-00450-9
39. F.A. Sabet, A. Raeisi Najafi, E. Hamed and I. Jasiuk: Modelling of bone fracture and strength at different length scales: a review(2042–8898 (Print)).
40. M. Figueiredo, J. Gamelas, A. Martins, Characterization of bone and bone-based graft materials using FTIR spectroscopy. Infrared Spectrosc-life Biomed. Sci. (2012). https://doi.org/10.5772/36379
41. H. Follet, G. Boivin, C. Rumelhart, P.J. Meunier, The degree of mineralization is a determinant of bone strength: a study on human calcanei. Bone **34**(5), 783 (2004)
42. L. Wang, J. Kang, C. Sun, D. Li, Y. Cao, Z. Jin, Mapping porous microstructures to yield desired mechanical properties for application in 3D printed bone scaffolds and orthopaedic implants. Mater. Design **133**, 62 (2017)
43. E.G. Choubar, M.H. Nasirtabrizi, F. Salimi, N. Sohrabi-gilani, A. Sadeghianamryan, Fabrication and in vitro characterization of novel co-electrospun polycaprolactone/collagen/polyvinylpyrrolidone nanofibrous scaffolds for bone tissue engineering applications. J. Mater. Res. (2022). https://doi.org/10.1557/s43578-022-00778-w
44. S. Mohammadi, S.S. Shafiei, M. Asadi-Eydivand, M. Ardeshir, M. Solati-Hashjin, Graphene oxide-enriched poly (ε-caprolactone) electrospun nanocomposite scaffold for bone tissue engineering

applications. J. Bioactive and Compatible Polym. **32**(3), 325 (2017)
45. L. Zhang, K. Pan, S. Huang, X. Zhang, X. Zhu, Y. He, X. Chen, Y. Tang, L. Yuan, D. Yu, Graphdiyne oxide-mediated photodynamic therapy boosts enhancive T-cell immune responses by increasing cellular stiffness. Int. J. Nanomed. (2023). https://doi.org/10.2147/IJN.S392998
46. C. Sandino, D. Lacroix, A dynamical study of the mechanical stimuli and tissue differentiation within a CaP scaffold based on micro-CT finite element models. Biomech Model Mech. **10**, 565 (2011)
47. D. Rowley: Bone repair biomaterials: JA Planell Pp. 478. New Delhi: Woodhead Publishing Ltd, 2009. ISBN: 978-1-84569-385-5.£ 145.00, (The British Editorial Society of Bone and Joint Surgery, City, 2010).
48. S.A.-O. Chu, H. Xu, X. Li, T. Guo, Z. Ting and Y. Zhou: Application of modified alveolar ridge augmentation technique for horizontal bone augmentation in posterior mandibular region: Report of 3 cases(2050-0904 (Print)).
49. A. Manke, L. Wang, Y. Rojanasakul, Mechanisms of nanoparticle-induced oxidative stress and toxicity. BioMed Res. Int. (2013). https://doi.org/10.1155/2013/942916
50. G. Turnbull, J. Clarke, F. Picard, P. Riches, L. Jia, F. Han, B. Li and W. Shu: 3D bioactive composite scaffolds for bone tissue engineering(2452-199X (Electronic)).
51. G. Zhu, T. Zhang, M. Chen, K. Yao, X. Huang, B. Zhang, Y. Li, J. Liu, Y. Wang, Z. Zhao, Bone physiological microenvironment and healing mechanism: Basis for future bone-tissue engineering scaffolds. Bioactive Mater. **6**(11), 4110 (2021)
52. P. Feng, P. Wei, P. Li, C. Gao, C. Shuai, S. Peng, Calcium silicate ceramic scaffolds toughened with hydroxyapatite whiskers for bone tissue engineering. Mater. Character. **97**, 47 (2014)
53. X. Wu, K. Walsh, B.L. Hoff, G. Camci-Unal, Mineralization of biomaterials for bone tissue engineering. Bioengineering **7**(4), 132 (2020)
54. E. Steijvers, A. Ghei and Z. Xia: Manufacturing artificial bone allografts: a perspective(2096-112X (Electronic)).
55. B.B. Rothrauff, R.S. Tuan, Decellularized bone extracellular matrix in skeletal tissue engineering. Biochem. Soc. Trans. **48**(3), 755 (2020)
56. G. Chen, Y. Lv, Decellularized bone matrix scaffold for bone regeneration. Decellularized scaffolds organogenesis Meth Proto (2018). https://doi.org/10.1007/7651_2017_50
57. K.E. Benders, P.R. Van Weeren, S.F. Badylak, D.B. Saris, W.J. Dhert, J. Malda, Extracellular matrix scaffolds for cartilage and bone regeneration. Trends Biotechnol. **31**(3), 169 (2013)
58. A. Pintor, L. Queiroz, R. Barcelos, L. Primo, L. Maia, G. Alves, MTT versus other cell viability assays to evaluate the biocompatibility of root canal filling materials: a systematic review. Int. Endodontic J. **53**(10), 1348 (2020)
59. F. Kouhestani, F. Dehabadi, M. Hasan Shahriari, S.R. Motamedian, Allogenic vs. synthetic granules for bone tissue engineering: an in vitro study. Prog. Biomater. **7**, 133 (2018)
60. F. Barrere, T. Mahmood, K. De Groot, C. Van Blitterswijk, Advanced biomaterials for skeletal tissue regeneration: instructive and smart functions. Mater. Sci. Eng. R: Rep. **59**(1–6), 38 (2008)
61. R.A. Perez, G. Mestres, Role of pore size and morphology in musculo-skeletal tissue regeneration. Mater. Sci. Eng: C **61**, 922 (2016)
62. J. Zeltinger, J.K. Sherwood, D.A. Graham, R. Müeller, L.G. Griffith, Effect of pore size and void fraction on cellular adhesion, proliferation, and matrix deposition. Tissue Eng. **7**(5), 557 (2001)
63. Y. Kuboki, Q. Jin, H. Takita, Geometry of carriers controlling phenotypic expression in BMP-induced osteogenesis and chondrogenesis. JBJS **83**(1), S105 (2001)
64. T.I. Shaheen, A. Montaser, S. Li, Effect of cellulose nanocrystals on scaffolds comprising chitosan, alginate and hydroxyapatite for bone tissue engineering. Int. J. Biol. Macromol. **121**, 814 (2019)
65. S. Bhumiratana, W.L. Grayson, A. Castaneda, D.N. Rockwood, E.S. Gil, D.L. Kaplan, G. Vunjak-Novakovic, Nucleation and growth of mineralized bone matrix on silk-hydroxyapatite composite scaffolds. Biomaterials **32**(11), 2812 (2011)
66. S. Samavedi, A.R. Whittington, A.S. Goldstein, Calcium phosphate ceramics in bone tissue engineering: a review of properties and their influence on cell behavior. Acta Biomaterialia **9**(9), 8037 (2013)
67. J. Ryu, S.H. Ku, H. Lee, C.B. Park, Mussel-inspired polydopamine coating as a universal route to hydroxyapatite crystallization. Adv. Funct. Mater. **20**(13), 2132 (2010)
68. H.-J. Park, J.-H. Choi, M.-H. Nam, Y.-K. Seo, Induced neurodifferentiation of hBM-MSCs through activation of the ERK/CREB pathway via pulsed electromagnetic fields and physical stimulation promotes neurogenesis in cerebral ischemic models. Int. J. Mol. Sci. **23**(3), 1177 (2022)